Adsorption of Methyl Violet 2B Dye by Silica from Glass Bottle Waste

Yatim Lailun Ni'mah[1*], Muhammad Zidan Chisa Faqih[1], Suprapto Suprapto[1], Nabila Eka Yuningsih[1], and Nor Laili-Azua Jamari[2]

[1]*Department of Chemistry, Faculty of Science and Data Analytics, Institut Teknologi Sepuluh Nopember, Kampus ITS Sukolilo, Surabaya 60111, Indonesia*

[2]*Department of Chemistry and Biology, Center for Defence Foundation Studies, National Defence University of Malaysia, Kem Sungai Besi, Kuala Lumpur 57000, Malaysia*

* ***Corresponding author:***

tel: +62-85732108646
email: yatimnikmah@gmail.com

Received: August 24, 2025
Accepted: September 26, 2025

DOI: 10.22146/ijc.110644

Abstract: *In this study, silica gel was successfully synthesized using waste from chemical reagent glass bottles. The synthesized silica gel was then tested for its effectiveness to adsorp methyl violet 2B dye. To optimize the adsorption process, surface response methodology (RSM) was employed, utilizing the Box-Behnken design (BBD) for factor and input design. Characterization of the synthesized silica gel through XRD analysis revealed an amorphous structure and mesoporous pores, with a purity of 75.63%. The optimization process focused on four key factors: pH (3 to 9), initial concentration of methyl violet 2B (10 to 30 mg/L), adsorbent mass (30 to 100 mg), and contact time (15 to 60 min). The optimal conditions for adsorbing methyl violet 2B were determined to be a pH range of 7–9, an initial methyl violet 2B concentration of 27–30 mg/L, an adsorbent mass of 70–95 mg, and a contact time of 30–40 min. Under these optimized conditions, the methyl violet 2B removal efficiency of 98.69% was achieved. Further analysis indicated that the adsorption of methyl violet 2B onto the synthesized silica gel followed the Temkin isotherm and pseudo-second-order kinetics models.*

Keywords: *adsorption; Box-Behnken design; methyl violet 2B; response surface methodology; silica gel*

■ INTRODUCTION

The accumulation of solid waste poses a significant challenge for many countries worldwide, driven by factors such as uncontrolled population growth, urbanization, and modernization [1]. According to World Bank data in 2018, Indonesia stands out as the fifth-largest producer of solid waste globally, generating a staggering 65.2 billion metric tons, and is the leading producer of solid waste in Southeast Asia [2]. In Indonesia, organic waste, paper waste, and glass waste are the primary contributors to this solid waste burden [3]. The accumulation of glass waste raises significant concern for Indonesia's environmental future. As a non-biodegradable material, glass waste poses a significant threat, potentially depleting the landfill space and resulting in severe environmental pollution [4]. Indonesia generates approximately 0.7 tons of glass waste per year, with chemical reagent glass bottles being the common glass waste type found [5]. Consequently, it is imperative to manage and treat glass waste, including chemical reagent glass bottle waste, in an appropriate manner to prevent environmental contamination [6].

Efforts to find innovative solutions for the efficient utilization of glass waste have led to various initiatives. These include incorporating glass waste into cement and concrete mixtures [4], utilizing it as a material for pavement coating and as an ingredient in asphalt mixtures [7], and employing it in the synthesis of silica gel [5,8]. Glass waste can be utilized in the synthesis of silica gel due to its relatively high silica content, typically ranging from 65 to 75% [6]. Consequently, glass bottle waste holds the potential to be processed and transformed into sodium silicate, which serves as a precursor for silica gel production [8]. The resulting

silica gel can be applied in various applications, including its use as an adsorbent for synthetic dye waste [9].

Synthetic dye waste is classified as hazardous and toxic due to its detrimental effects on the environment [10]. The disposal of synthetic dye waste in water bodies, such as rivers or oceans, can lead to severe environmental consequences, particularly for aquatic ecosystems. These impacts include the obstruction of sunlight penetration into the water, inhibition of bacterial growth, disruption of photosynthesis in aquatic plants, and reduction of dissolved oxygen levels [11]. Moreover, many synthetic dyes are known to be carcinogenic and teratogenic to humans, making them extremely dangerous if these contaminants enter the drinking water supplies [12].

Methyl violet 2B, which belongs to the triphenylmethane cationic dye group, is a synthetic dye widely used in various industries, including textiles, paper, plastics, paints, coatings, pharmaceuticals, and cosmetics [13]. This dye exhibits high solubility in water and a strong affinity for compounds such as ethanol, diethylene glycol, and triethylene glycol [11]. Methyl violet 2B is commonly used to impart purple color to paints and inks, as well as for dyeing materials such as cotton, paper, silk, bamboo, leather, and straw [13-14].

Methyl violet 2B dye poses significant health effects, including eye and skin irritation, respiratory tract irritation, digestive tract irritation if accidentally inhaled or ingested, accelerated heart rate, vomiting, shock, and jaundice (cyanotic jaundice) [14-16]. Considering these potential risks, the removal of synthetic dyes from textile wastewater becomes a crucial aspect of wastewater treatment processes. The use of methyl violet 2B in industry produces hazardous and toxic liquid waste, so it needs to be treated first before being discharged into the environment and meeting the quality standard threshold [14].

To address this challenge, various methods have been employed to remove dyes from wastewater, including ozonation [17], coagulation-flocculation [18], membrane filtration [19], electrochemical oxidation [20], photocatalytic oxidation [21], and adsorption [22]. Among these methods, adsorption has demonstrated effectiveness in removing or reducing dye levels in wastewater [14] due to its simplicity, high performance, and relatively low application costs [23].

To ensure optimal performance of the adsorption process for waste treatment, it is crucial to utilize an adsorbent with a high adsorption capacity. Silica gel is a promising material for adsorbing pollutants in water due to its reactive surface-containing silanol (Si–OH) groups, and its pore channels that enable selective adsorption with the adsorbate [9]. Moreover, silica gel exhibits excellent characteristics such as high porosity (> 90%) and a relatively large specific surface area (500–1,000 m^2/g). The efficacy of silica gel as a dye adsorbent has been demonstrated in various studies. Chen et al. [24] found that heat-treated silica gel at 500 °C displayed a maximum adsorption capacity of 437.2 mg/g for Congo red dye and 428.8 mg/g for methylene blue dye. In another study, Han et al. [25] reported that surface-modified silica gel exhibited a maximum adsorption capacity of 65.74 mg/g for methylene blue dye and 185.61 mg/g for rhodamine B dye. Based on these findings, the adsorption potential of silica gel derived from chemical reagent glass bottle waste for the removal of methyl violet 2B dye was investigated in this study.

In this research, the optimization of adsorption parameters was performed using the response surface methodology (RSM) with the Box-Behnken design (BBD) as an experimental design. RSM offers advantages over the one-factor-at-a-time (OFAT) method, including a reduced number of experiments, the ability to explore interactions between variables, cost-effectiveness, and time efficiency [26]. BBD was chosen as the experimental design due to its ability to achieve reliable results with a reduced number of experiments compared to other designs [27]. The adsorption parameters investigated in this study include pH, initial concentration of the adsorbate solution, contact time, and adsorbent mass. To elucidate the mechanism and capacity of methyl violet 2B adsorption, adsorption isotherm models and kinetics were employed in this study.

■ EXPERIMENTAL SECTION

Materials

The materials used in this research were a chemical

reagent glass bottle (brown glass), NaOH (98% purity, Merck, Germany), aqua DM, HCl (37%, Merck), and methyl violet 2B (p.a., SAP chemical).

Instrumentation

The instruments used in this research were a disc mill, a wire mesh sieve 63–74 μm, a hot plate, a muffle furnace, oven, UV-vis spectrophotometer (Genesys 10S), X-ray diffraction (XRD, XPERT-PRO), Fourier transform infra-red (FTIR, Shimadzu Instrument Spectrum One 8400S) and X-ray fluorescence (XRF, Rigaku ZSX Primus IV).

Procedure

Synthesis of silica gel

Silica gel from chemical reagent glass bottle waste was synthesized by following the method described in our previous study [5]. Firstly, the powdered waste was mixed with NaOH in a crucible at a weight ratio of 1:3 (glass powder to NaOH, w/w). The mixture was then calcinated in a furnace at 800 °C for 4 h, resulting in the formation of solid sodium silicate. The solid sodium silicate was subsequently dissolved in boiling distilled water, and the mixture was allowed to stand until two distinct phases were formed. The mixture was then filtered using Whatman filter paper, yielding a filtrate that was utilized in the subsequent silica synthesis process [6].

Then, the filtrate was slowly dripped into a solution of 3 M HCl while continuously stirring at a speed of 450 rpm. This process continued until a white gel was formed at a pH range of 0.2–2.0. The resulting gel was left at room temperature for 18 h and subsequently filtered using Whatman filter paper No. 42. The filtered gel was then washed with aqua DM until it reached a neutral pH of 6 to 7. After that, the gel was dried in an oven at 80 °C for 12 h to obtain dry silica gel. The resulting dry silica gel was weighed to determine its mass [8].

Characterization of synthesized silica gel

The synthesized silica gel's structure was analyzed using XRD. The sample was subjected to a scanning process within an angular range of 10° to 80°, using Cu-Kα radiation with a wavelength (k-value) of 1.5406 Å. This allowed for the determination of the crystalline structure and identification of diffraction patterns (if any) present in the synthesized silica gel. To identify the functional groups present in the synthesized silica gel, FTIR spectroscopy analysis was employed. This spectroscopic technique enabled the detection and analysis of the characteristic absorption bands associated with various functional groups within the silica gel sample. The purity and elemental composition of the synthesized silica gel were assessed using XRF analyzer. This analytical instrument provided information about the relative abundance and distribution of different elements present in the synthesized silica gel. Furthermore, adsorption desorption N_2 (Quantachrome Autosorb IQ, USA) was utilized to determine the specific surface area and pore size distribution of the synthesized silica gel.

Adsorption experiments

The adsorption study was conducted using the batch method. In this method, 20 mL of methyl violet 2B solution with a specific initial concentration and pH was mixed with a predetermined quantity of silica gel in a glass beaker at room temperature. Adjustment to pH 3, 6, and 9 by adding 0.1 M HCl for acidic conditions and 0.1 M NaOH for basic conditions. The mixture was then stirred at a speed of 450 rpm. Various parameters that influence the adsorption process, including pH, adsorbent mass, methyl violet 2B solution concentration, and contact time, were investigated using the BBD approach. The BBD design utilized in this study involved three levels (−1, 0, and +1) for each parameter. The pH range examined was 3 to 9, the adsorbent mass varied from 30 to 100 mg, the solution concentration ranged from 10 to 30 mg/L for 20 mL, and the contact time spanned from 15 to 60 min. The parameter levels and their ranges are summarized in Table 1.

The adsorption experiments were designed according to the BBD, and a total of 27 adsorption experiments were conducted in this study to investigate the influence of pH, adsorbent amount, adsorbate solution concentration, and contact time on the adsorption of methyl violet 2B dye using synthesized silica gel. The effectiveness of the adsorption process was evaluated by calculating the percentage of dye removal. The specific combinations of the experimental parameters have 27 experiments.

Table 1. Adsorption parameter and level

Parameters	Level		
	−1	0	+1
pH	3	6	9
Adsorbent mass (mg)	30	50	100
The concentration of methyl violet 2B solution (mg/L)	10	20	30
Contact time (min)	15	30	60

Following the completion of the adsorption process, the mixture containing silica gel and methyl violet solution was subjected to centrifugation at 3000 rpm for 15 min to separate the residue from the solution of methyl violet. Subsequently, a small aliquot of the supernatant was taken, and its absorbance was measured at the maximum wavelength (584–585 nm) using a UV-vis spectroscopy to determine the amount of methyl violet that remained unadsorbed. The percentage removal value, as well as the amount of methyl violet 2B adsorbed at each time point (q_t) and equilibrium (q_e), were calculated using Eq. (1–3) [14].

$$\%\,\text{Removal} = \frac{(C_0 - C_t)}{C_0} \times 100\% \quad (1)$$

$$q_t = \frac{(C_0 - C_t)}{m} \times V \quad (2)$$

$$q_e = \frac{(C_0 - C_e)}{m} \times V \quad (3)$$

The variables C_0, C_t, and C_e represent the initial concentration of methyl violet, the concentration of methyl violet at a given time (t), and the concentration of methyl violet at equilibrium (mg/L), respectively. The variables m and V denote the weight of the silica gel adsorbent used (g) and the volume of the methyl violet solution (L), respectively.

The relationship between the data on methyl violet removal and the adsorption parameters can be mathematically expressed using a second-order polynomial, as demonstrated by Eq. (4) [28].

$$y = \beta 0 + \sum_{j=1}^{k} \beta_j X_j + \sum_{j=1}^{k} \beta_{jj} X_j^2 + \sum \sum_{i<j=2}^{k} \beta_{ij} X_i X_j \quad (4)$$

According to Eq. (4), y represents the response function, 0 denotes the constant coefficient, j, jj, and ij represent the linear, quadratic, and interaction terms between variables, and X_i and X_j represent the levels of the independent variables [29]. By utilizing Eq. (4), the collected data is processed and visualized in a three-dimensional (3D) surface plot. This plot illustrates the effect of each parameter on the percentage removal value and highlights the interactions between the parameters. Through analysis of the resulting plots, the optimal conditions and performance for the adsorption of methyl violet by the synthesized silica gel can be determined and evaluated.

Adsorption isotherm and kinetics studies

The adsorption isotherm for methyl violet 2B onto silica adsorbent was determined by fitting the experimental data of varying concentration (10, 15, 20, 25, and 30 ppm) to various isotherm models. The experimental data were collected from the adsorption experiment using optimal conditions derived from the polynomial equation of RSM analysis. Other factors such as pH, adsorbate volume, adsorbent mass, and contact time were kept at their optimal levels during the experiments. The concentration of the methyl violet 2B at equilibrium (C_e) and the amount of methyl violet 2B adsorbed at equilibrium (q_e) were then used to determine the adsorption isotherm model by plotting them on the Langmuir, Freundlich, and Temkin isotherm equations, as shown in Table 2.

Similarly, for evaluating the adsorption kinetics model, the contact time varied at 15, 20, 25, 30, and 35 min while maintaining the pH, amount of adsorbent, and initial concentration of methyl violet solution at their optimal settings. The collected data included the time data (t) and the amount of methyl violet 2B adsorbed at each time point (q_t) were used to determine the kinetics model for methyl violet adsorption by fitting the data to the pseudo-first-order and pseudo-second-order equations, as shown in Table 2.

Table 2. Adsorption isotherms and kinetics model equations

Isotherms and kinetics model	Equations	Reference
Langmuir	$\frac{C_e}{q_e}=\frac{C_e}{q_0}+\frac{1}{q_0\cdot K_L}$ $R_L=\frac{1}{1+K_L\cdot C_0}$	[29]
(Cont*) Freundlich	$\ln q_e=\frac{1}{n}\ln C_e+\ln K_f$	[30]
Temkin	$q_e=\frac{RT}{b}\ln K_T+\frac{RT}{b}\ln C_e$	[31]
Pseudo-first-order	$\log(q_e-q_t)=\log q_e-k_1 t$	[29]
Pseudo-second-order	$\frac{t}{q_t}=\frac{1}{k_2 q_e^2}+\frac{t}{q^e}$	[32]

where C_e (mg/L) is the adsorbate concentration at equilibrium; q_e (mg/g) is the amount of methyl violet 2B adsorbed at equilibrium; q_0 (mg/g) is the adsorption capacity of the adsorbent; q_t (mg/g) is the amount of methyl violet 2B adsorbed at time, t (min); K_L (L/mg) is the Langmuir adsorption constant; R_L is the adsorption rate; K_f is the Freundlich adsorption constant; A and B are Temkin constants; k_1 is the pseudo-first-order rate constant; and k_2 is the pseudo-second-order rate constant

■ RESULTS AND DISCUSSION

Synthesis and Characterization of Silica Gel

In this study, the silica gel was synthesized by combining two methods (alkaline fusion and sol-gel), which were conducted by Ni'mah et al. [5] and Owoeye et al. [8], respectively. Initially, the silica present in the glass bottle waste powder was extracted using NaOH and high temperatures through the alkaline fusion method. Subsequently, the extracted silica, in the form of sodium silicate, underwent a conversion process to transform it into silica gel via the sol-gel method.

The characterization of the synthesized silica gel was conducted using XRD, FTIR, XRF, and the BJH Method. The data obtained from these analyses are presented in Fig. 1(a–c) and Table 3. Fig. 1(a) represents the diffractogram of the synthesized silica gel. The broad peaks observed in the angle range of 20° to 27° indicate the amorphous nature of the silica gel. This finding aligns with the research conducted by Ni'mah et al. [5], which found that amorphous silica gel is characterized by a broadened peak within the same angle range.

The FTIR spectrum of the synthesized silica gel is depicted in Fig. 1(b), and several characteristic bands for silica gel are observed in the spectrum. For instance, the band at a wavenumber of 550 cm^{-1} corresponds to the siloxane (Si–O–Si) ring. Additionally, bands at wavenumbers 679, 797, and 1090 cm^{-1} correspond to the bending, symmetric stretching, and asymmetric stretching vibrations of the Si–O–Si groups, respectively. The presence of Si–OH groups in the synthesized silica gel is shown by the band at 961 cm^{-1}, which further confirms its identity as silica gel. Apart from that, the band with wavenumber 1636 cm^{-1}, which corresponds to the bending vibrations of the H–O–H groups, and

Table 3. XRF analysis result

Component	Quantity (%mass)
Na_2O	8.19
MgO	0.12
Al_2O_3	8.39
Fe_2O_3	0.54
SiO_2	75.63
Cl	0.71
K_2O	0.27
CaO	0.09
MnO	0.06
NiO	0.03
CuO	0.01

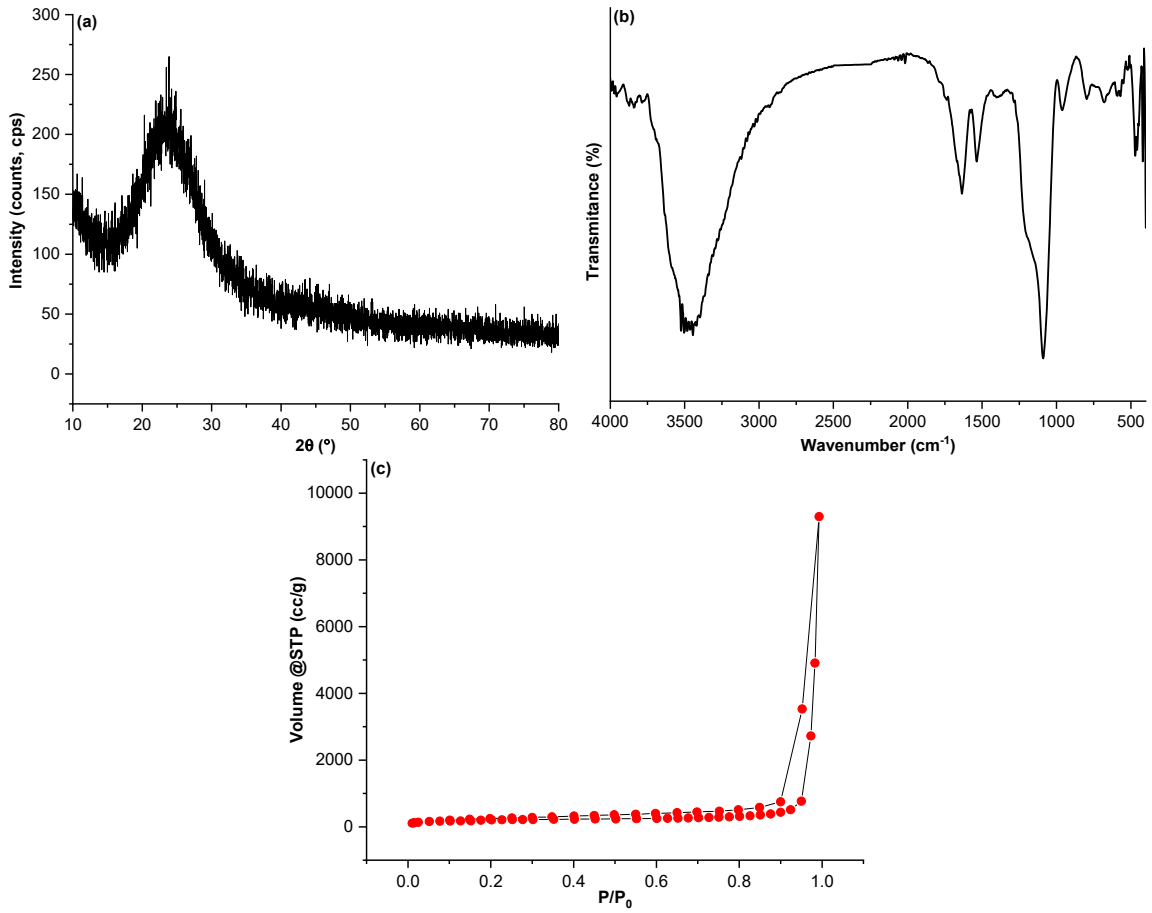

Fig 1. Silica gel characterization using (a) XRD, (b) FTIR, and (c) BJH methods

a broad band at wavenumber 3462 cm^{-1}, suggesting the presence of adsorbed water (H_2O) on the silica gel.

Fig. 1(c) displays the results of pore analysis conducted on the surface of the synthesized silica gel using N_2 adsorption-desorption. The graph indicates that the N_2 adsorption-desorption follows the type IV isotherm model, indicating a mesoporous structure of the synthesized silica gel. Further analysis using the BJH method reveals a pore size with a diameter of 15.74 nm and a specific surface area of 298.083 m^2/g. Table 3 presents the results of the XRF analysis, providing the composition of the silica gel in terms of mass percentage (%mass). The analysis indicates that SiO_2 constitutes 75.63% of the total mass, confirming the purity of the synthesized silica gel.

Adsorption Analysis

A total of 27 experiments were carried out in this study to optimize the adsorption of methyl violet 2B by optimizing four key parameters: pH, initial concentration of methyl violet 2B solution, adsorbent mass, and contact time. The experimental design matrix, as well as the experimental and predicted results shown in percentage removal values, are presented in Table 4. The results of the regression analysis (Table 5) reveal a correlation coefficient (R^2) of 0.7940, indicating a significant correlation between the experimental response value and the predicted response value [33]. Additionally, the regression analysis results show that the experimental data groups have a P-value of 0.0224, which is less than 0.05, indicating that the input variables significantly affect the response.

The collected data were then subjected to regression analysis to determine the correlation model. Through this analysis, a set of regression results was obtained, along with a polynomial equation that represents the relationship between the input variables (pH, initial concentration of methyl violet 2B solution,

Table 4. Adsorption experiment result

Experiment	Parameters				%Removal	%Predicted removal
	pH	Adsorbent mass (mg)	The initial concentration of MV (mg/L)	Contact time (min)		
1	3	50	20	15	90.9435	93.0625
2	9	50	20	15	98.1397	98.3140
3	3	50	20	60	91.7964	92.2859
4	9	50	20	60	99.3657	98.8828
5	3	30	20	30	88.8646	91.1141
6	9	30	20	30	98.5661	99.1477
7	3	100	20	30	98.6727	97.4747
8	9	100	20	30	99.2058	97.3406
9	3	50	10	30	97.1322	94.2101
10	9	50	10	30	97.2388	96.9428
11	3	50	30	30	92.8607	92.1228
12	9	50	30	30	98.9019	100.7901
13	6	30	20	15	98.4062	96.2886
14	6	30	20	60	97.3934	96.3497
15	6	100	20	15	98.0330	98.7579
16	6	100	20	60	97.8731	98.2416
17	6	50	10	15	97.0256	97.2015
18	6	50	10	60	95.2132	95.8606
19	6	50	30	15	98.3333	97.2568
20	6	50	30	60	98.3689	98.3900
21	6	30	10	30	94.8934	95.9477
22	6	100	10	30	97.8785	99.2190
23	6	30	30	30	98.1201	97.3960
24	6	100	30	30	98.0490	98.6782
25	6	50	20	30	98.6194	98.5128
26	6	50	20	30	98.5661	98.5128
27	6	50	20	30	98.3529	98.5128

adsorbent mass, and contact time) and the response (%removal value). The correlation polynomial equation is presented in Eq. (5).

$$\begin{aligned} Y = {} & 75.969 + 0.276x_0 - 0.073x_1 + 0.062x_2 + 3.475x_3 \\ & - 0.001{x_0}^2 - 0.001x_0x_1 - 0.0001x_0x_2 - 0.019x_0x_3 \\ & - 0.004{x_1}^2 + 0.003x_1x_2 + 0.049x_1x_3 - 0.002{x_2}^2 \\ & + 0.005x_2x_3 - 0.224{x_3}^2 \end{aligned} \quad (5)$$

Eq. (5) represents the correlation between the response value (%removal), denoted as y and the input variables. The input variables are as follows: x_0 corresponds to the adsorbent mass, x_1 represents the initial concentration of methyl violet 2B solution, x_2 represents the contact time, and x_3 represents the pH.

Fig. 2 displays the stem plot of residuals, which represent the differences in percentage removal between the experimental and predicted values. The percentage removal gaps between each experimental and its corresponding predicted value are relatively small, indicating that the experimental model employed in this study is consistent [5]. Furthermore, the distribution of residuals in Fig. 3 shows that the residual data in this study follow a normal distribution.

The response surface curves in Fig. 4(a–f) provide a clearer representation of the interaction between the input variables and the response. Fig. 4(a) specifically illustrates the relationship between the mass of the silica

Table 5. Regression analysis result

Dep. Variable:	Removal	R-squared:	0.794			
Model:	OLS	Adj. R-squared:	0.553			
Method:	Least Square	F statistic:	3.302			
Date:	Friday, 30 Dec 2022	Prob (F-statistic):	0.0224			
Time:	17:13:23	log-Likelihood:	−43.534			
Observation No.:	27	AIC:	117.1			
Df Residual:	12	BIC:	136.5			
Df Model:	14					
Covariance type:	nonrobust					
Coeff.	std	err	t	P>|t|	0.025	0.975
Const.	75.9689	10.355	7.337	0.000	53.408	98.530
x_1	0.2758	0.136	2.030	0.065	−0.020	0.572
x_2	−0.0731	0.414	−0.177	0.863	−0.975	0.828
x_3	0.0621	0.189	0.329	0.748	−0.349	0.473
x_4	3.4753	1.379	2.520	0.027	0.470	6.480
x_5	−0.0007	0.001	−0.870	0.402	−0.002	0.001
x_6	−0.0014	0.002	−0.578	0.574	−0.007	0.004
x_7	−0.0002	0.001	−0.174	0.865	−0.002	0.002
x_8	−0.0194	0.008	−2.375	0.035	−0.037	−0.002
x_9	−0.0048	0.008	−0.606	0.556	−0.022	0.012
x_{10}	0.0027	0.004	0.704	0.495	−0.006	0.011
x_{11}	0.0495	0.030	1.630	0.129	−0.017	0.116
x_{12}	−0.0019	0.002	−1.041	0.318	−0.006	0.002
x_{13}	0.0050	0.013	0.383	0.709	−0.023	0.033
x_{14}	−0.2243	0.088	−2.561	0.025	−0.415	−0.033
Omnibus:	0.735	Durbin-Watson:	1.673			
Prob (Omnibus):	0.692	Jarque-Bera (JB):	0.352			
Skew:	0.279	Prob (JB):	0.839			
Kurtosis:	2.974	Cond. No. 1.71e+05				

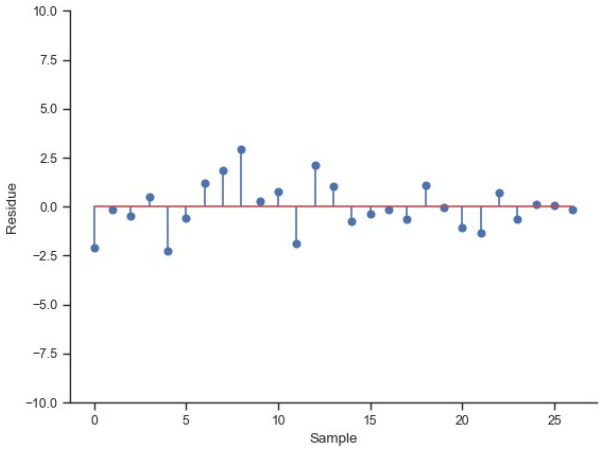

Fig 2. The stem plot of residual

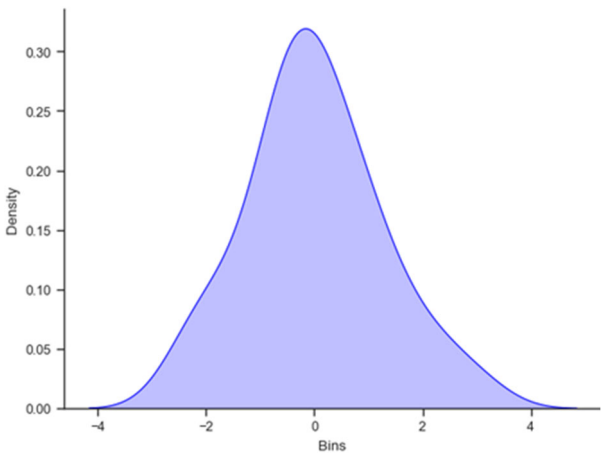

Fig 3. Residual distribution

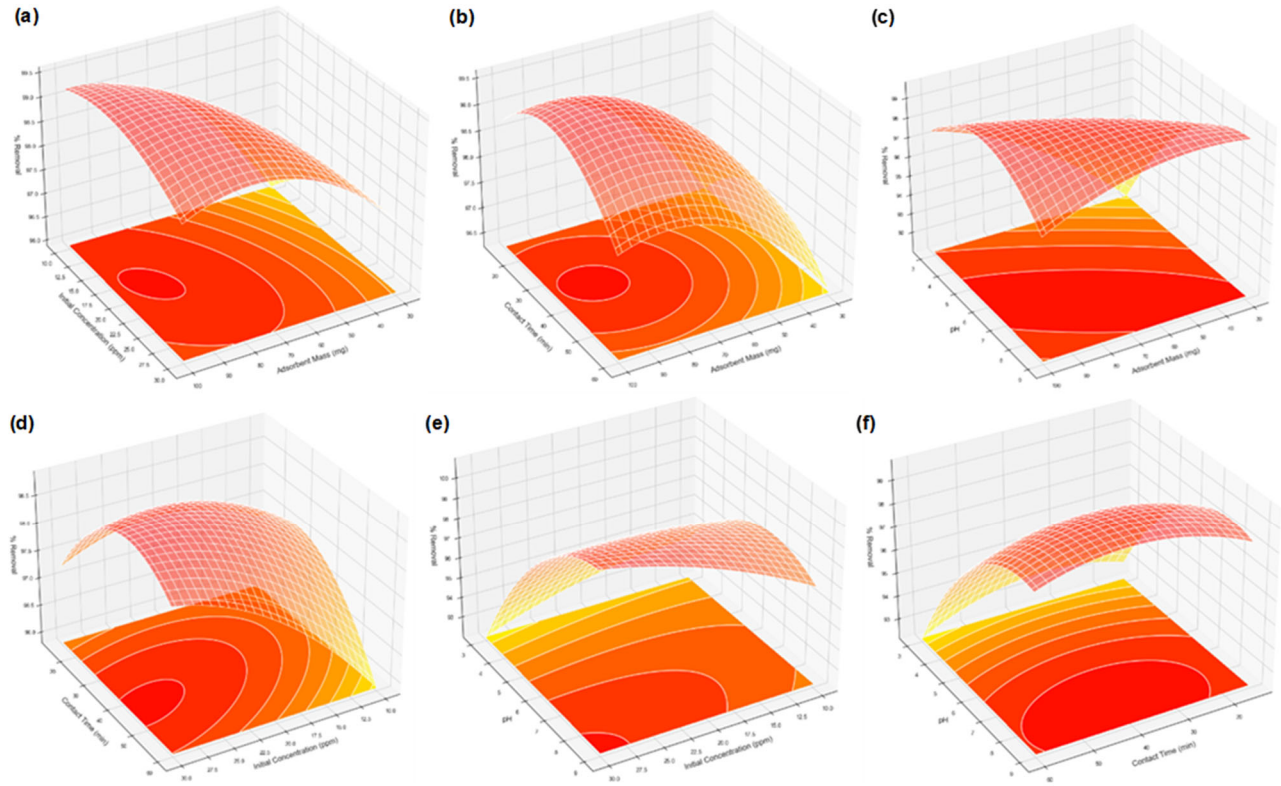

Fig 4. Response surface (3-D) shows the effect of %removal on (a) initial concentration vs. adsorbent mass, (b) contact time vs. adsorbent mass, (c) pH vs. adsorbent mass, (d) contact time vs initial concentration, (e) pH vs initial concentration, and (f) pH vs. contact time

gel adsorbent, the initial concentration of the methyl violet 2B solution, and the percentage removal value of the dye. By examining the contours on the surface curve, it is evident that the percentage removal of methyl violet 2B increases with an increase in the adsorbent mass, while it decreases with an increase in the initial concentration of the methyl violet 2B solution. The optimal percentage removal of methyl violet is achieved within the range of 80–95 mg for the adsorbent mass and 16.0–21.0 mg/L for the concentration of the methyl violet 2B solution.

This finding aligns with the theory that increasing adsorbent mass results in a higher percentage removal in dye adsorption. This is because more active adsorption sites are available in the adsorbent-adsorbate system, enabling the adsorption of more dye molecules. Conversely, increasing the initial concentration of the adsorbate solution decreases the percentage removal. This occurs because higher dye concentrations mean more dye molecules in the system, causing the adsorbent surface to become saturated more rapidly by the dye molecules [31].

Fig. 4(b) shows the surface curve illustrating the relationship between adsorbent mass, contact time, and the percentage removal of methyl violet 2B. The contour plot on this surface indicates that the percentage removal of methyl violet increases with higher adsorbent mass and longer contact time. Optimal conditions are found within the range of 78–95 mg for adsorbent mass and 27–40 min for contact time. The increase in percentage removal with longer contact time is due to the extended agitation (stirring) of the adsorbent-adsorbate system. Increasing the stirring time provides the energy needed for methyl violet 2B dye molecules to move through the solution and reach the active sites on the adsorbent, thereby enhancing the chances for direct contact between the dye molecules and the active adsorption sites. As a result, more molecules can bind to the active sites as contact time increases. However, if contact time continues to grow, all active sites gradually become saturated with dye molecules, causing the adsorption rate to decline until equilibrium is achieved at a certain point [11].

The relationship between adsorbent mass, pH, and the percentage removal of methyl violet 2B is illustrated in Fig. 4(c). The surface curve shows that optimal methyl violet 2B adsorption occurs within an adsorbent mass range of 30–100 mg and a pH range of 5–9. Notably, the curve indicates that even with an adsorbent mass of 30 mg, optimal adsorption can be achieved by maintaining the solution's pH at its optimal alkaline level. The pH conditions of the adsorbate-adsorbent system influence the electrostatic charge, ionization degree, and chemical properties of the adsorbent surface. Optimization studies on methyl violet adsorption parameters conducted by Sarkar et al. [11] confirm that the optimal pH for methyl violet adsorption falls within the alkaline range (pH > 7), specifically between pH 7 and 9. In acidic conditions (pH < 7), there is competition between H^+ ions in the solution and cationic methyl violet molecules to bind to the negatively charged active sites of the adsorbent. This reduces the number of available active sites for dye molecule adsorption. Conversely, in alkaline pH, OH^- ions in the solution increase the negative charge on the adsorbent surface, enhancing the electrostatic attraction between the adsorbent and the dye molecules. As a result, methyl violet dye adsorption increases [32].

Fig. 4(d) depicts the surface curve illustrating the relationship between the initial concentration of the methyl violet 2B solution, contact time, and the percentage removal of methyl violet 2B. The contour plot reveals that optimal adsorption occurs within the concentration range of 25.0–30.0 mg/L and the contact time range of 40–48 min. Fig. 4(e) demonstrates the relationship between pH, initial concentration of the methyl violet 2B solution, and the percentage removal of methyl violet. This figure illustrates that the optimal conditions for removal of methyl violet 2B are at a concentration of 27.5–30.0 mg/L and pH range of 8–9. In addition, Fig. 4(f), which displays the relationship between contact time, pH, and the percentage removal of methyl violet 2B, reveals that optimal methyl violet adsorption occurs within the pH range of 7–9 and the contact time range of 20–57 min.

Based on the observations from Fig. 4(a–f), it can be concluded that the optimal adsorption of methyl violet 2B dye by silica gel derived from chemical reagents glass bottle waste occurs at pH variations of 7–9, an initial concentration range of methyl violet 2B solution of 27.0–30.0 mg/L, an adsorbent mass range of 70–95 mg, and a contact time range of 30–40 min. To determine the theoretical optimum percentage removal value, the optimum data variations (pH of 9, initial concentration of methyl violet 2B solution of 27 mg/L, adsorbent mass of 95 mg, and contact time of 40 min) were input into the polynomial Eq. (5), and the value of 98.69% removal was obtained.

pH in the adsorption process has a very significant influence because it describes the interaction between methyl violet 2B and the SiO_2. pH affects the charge on SiO_2, where the silica surface can be ionized, the Si–OH group can be deprotonated to $Si–O^-$ at high pH or protonated to $Si–OH_2^+$ at low pH (Fig. 5). In acidic conditions (pH < 2), the silanol group on the silica surface is protonated ($Si–OH_2^+$), producing a positive charge. Because methyl violet 2B is also positively charged, the electrostatic interaction becomes weak or even repulsion occurs, thus reducing adsorption. In basic conditions, the silanol group will be deprotonated to $Si–O^-$, so that the silica surface becomes negatively charged. This will significantly enhance the electrostatic interaction with the methyl violet 2B molecule, thereby increasing the adsorption efficiency until the optimum pH is reached, resulting in maximum adsorption [32].

Adsorption Isotherm and Kinetics of Methyl Violet 2B on Synthesized Silica Gel

To determine the adsorption isotherm model, the optimized adsorption parameters (contact time of 40 min, pH 9, and adsorbent mass of 95 mg) were employed with various concentrations of methyl violet 2B solution (10, 15, 20, 25, and 30 mg/L). Fig. 6(a–c) illustrates the regression analysis results for the Langmuir, Freundlich, and Temkin isotherm models applied to methyl violet adsorption using synthesized silica gel. The correlation coefficients (R^2) for each isotherm model show that the R^2 from the Temkin model (0.9471) is the highest, followed by the Freundlich (R^2 = 0.8690) and Langmuir (R^2 = 0.4148) models. It can be concluded that the adsorption of methyl violet 2B onto

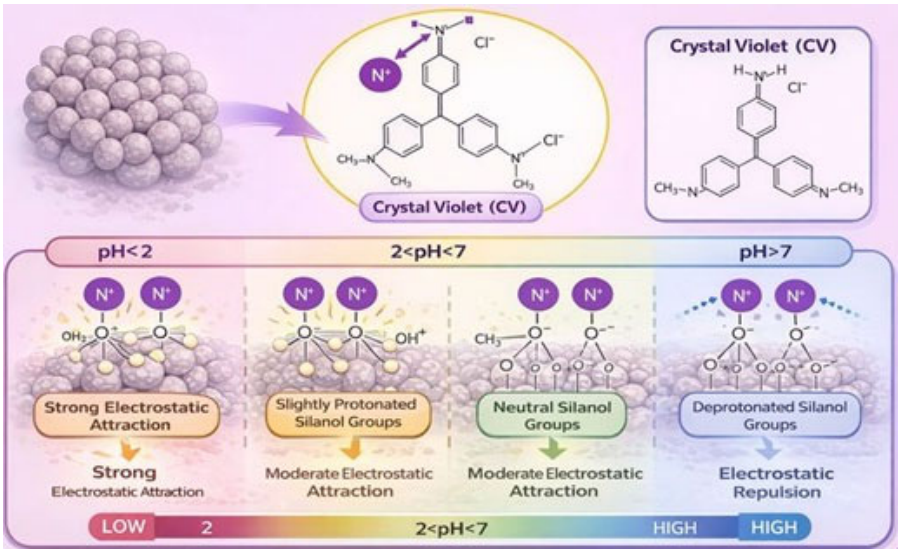

Fig 5. The effect of pH on the interaction between methyl violet 2B and SiO_2

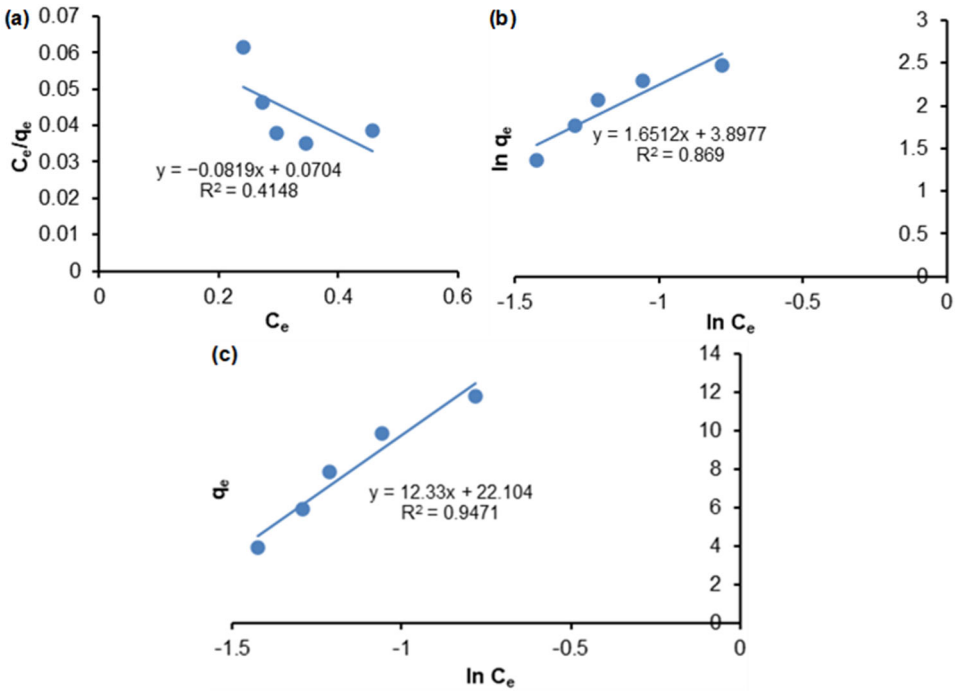

Fig 6. (a) Langmuir, (b) Freundlich, and (c) Temkin adsorption isotherm models of methyl violet 2B adsorption

synthesized silica gel follows the Temkin isotherm model, suggesting that the adsorption process occurs on multiple layers of the adsorbent surface (multilayer) and the heat of adsorption decreases linearly with increased surface coverage [34].

The kinetics isotherm model was also determined using the optimized adsorption parameters (methyl violet 2B solution concentrations of 27 mg/L, pH 9, and adsorbent mass of 95 mg) with different contact times ranging from 15 to 60 min (in 5-min intervals). The regressions of pseudo-first order and pseudo-second order kinetics adsorption models for methyl violet adsorption are presented in Fig. 7(a and b).

Based on the data presented in Fig. 6, it is evident that the R^2 pseudo-second-order model (0.999) is higher than the R^2 pseudo-first-order model (0.0033). This

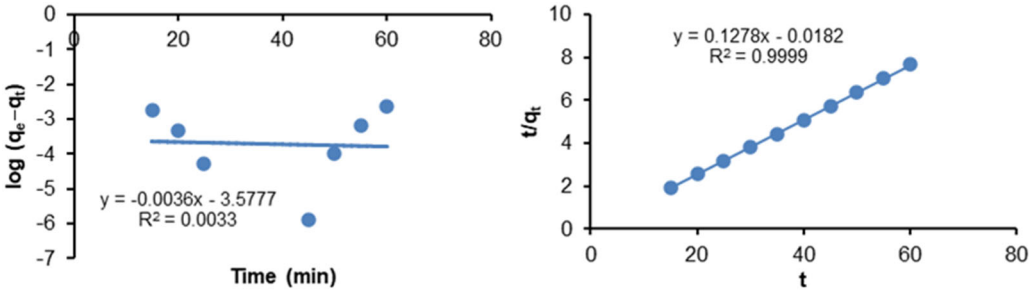

Fig 7. (a) Pseudo-first-order and (b) pseudo-second-order model of methyl violet 2B adsorption

suggests that the adsorption of methyl violet 2B onto synthesized silica gel follows the pseudo-second-order kinetics model, indicating that the ratio of accessible sites on the adsorbent to the rate of adsorption is linear. Co is the initial concentration of methyl violet 2B (mg/L); q_e and qt are the amount of methyl violet 2B adsorbed (mol/g) at equilibrium and at any time t (mol/g), respectively; k_1, k_2, k_3, and k_4 are the first-order (min^{-1}), second-order (g/mol min), pseudo-first-order (min^{-1}), and pseudo-second-order (g/mol min) adsorption rate constants, respectively. As shown in Fig. 7, the pseudo-second-order correlation coefficient is higher than the pseudo-first-order one. A higher correlation coefficient tends to follow the pseudo-second-order one. This indicates that the kinetic model is a chemical adsorption and does not involve mass transfer in solution. It is more likely to predict that adsorption involves possible electron sharing between the methyl violet 2B cations and the adsorbent [35]. Pseudo-second-order indicates that the adsorption process occurs through a chemical adsorption mechanism involving a strong reaction between the adsorbent and the adsorbate. Furthermore, the amount of solute on the adsorbent's surface influences the rate at which the reaction occurs [36].

■ CONCLUSION

By using RSM with BBD, the optimal conditions for methyl violet removal were identified as follows: pH range of 7–9, initial concentration range of 27.0–30.0 mg/L for 20 mL, adsorbent mass range of 70–95 mg, and contact time range of 30–40 min. The Temkin isotherm model showed the best fit to the experimental data, indicating multilayer adsorption with a decrease in heat of adsorption as surface coverage increased. Meanwhile, for adsorption kinetics, the pseudo-second-order model provided a superior fit, suggesting a linear relationship, that is, second-order kinetics indicates that the adsorption rate reflects physisorption. This is in line with the Temkin isotherm adsorption mechanism, namely, multilayer adsorption. Overall, the findings of this research contribute to the understanding of optimizing the adsorption process for methyl violet 2B dye using synthesized silica gel as an effective adsorbent. The identified optimal parameters can guide further applications in wastewater treatment and pollution mitigation.

■ ACKNOWLEDGMENTS

The authors gratefully acknowledge financial support from the Institut Teknologi Sepuluh Nopember for this work under the project scheme of the Publication Writing and IPR Incentive Program (PPHKI) 2026.

■ CONFLICT OF INTEREST

The authors declare that they have no known competing financial interests or personal relationships that could have appeared to influence the work reported in this paper.

■ AUTHOR CONTRIBUTIONS

Yatim Lailun Ni'mah: conceptualization, supervised the project, verified the analytical methods, validation, writing-review and editing. Muhammad Zidan Chisa Faqih: performed the experiments; paper drafting. Suprapto: experimental design, data analysis, and visualization. Nabila Eka Yuningsih: Validation, visualization and data analysis. Nor Laili-Azua Jamari: writing-review and editing.

■ REFERENCES

[1] Sajid, M., Raheem, A., Ullah, N., Asim, M., Ur Rehman, M.S., and Ali, N., 2022, Gasification of municipal solid waste: Progress, challenges, and prospects, *Renewable Sustainable Energy Rev.*, 168, 112815.

[2] Sondh, S., Upadhyay, D.S., Patel, S., and Patel, R.N., 2022, A strategic review on municipal solid waste (living solid waste) management system focusing on policies, selection criteria, and techniques for waste-to-value, *J. Cleaner Prod.*, 356, 131908.

[3] Kurniawan, T.A., Avtar, R., Singh, D., Xue, W., Dzarfan Othman, M.H., Hwang, G.H., Iswanto, I., Albadarin, A.B., and Kern, A.O., 2021, Reforming MSWM in Sukunan (Yogjakarta, Indonesia): A case-study of applying a zero-waste approach based on circular economy paradigm, *J. Cleaner Prod.*, 284, 124775.

[4] Poudel, S., Bhetuwal, U., Kharel, P., Khatiwada, S., KC, D., Dhital, S., Lamichhane, B., Yadav, S.K., and Suman, S., 2025, Waste glass as partial cement replacement in sustainable concrete: Mechanical and fresh properties review, *Buildings*, 15 (6), 857.

[5] Ni'mah, Y.L., Suprapto, S., Subandi, A.P.K., Yuningsih, N.E., and Pertiwi, A.C., 2022, The optimization of silica gel synthesis from chemical bottle waste using response surface methodology, *Arabian J. Chem.*, 15 (12), 104329.

[6] Ni'mah, Y.L., Subandi, A.P.K., and Suprapto, S., 2022, The application of silica gel synthesized from chemical bottle waste for zinc (II) adsorption using Response Surface Methodology (RSM), *Heliyon*, 8 (12), e11997.

[7] Ferdous, W., Manalo, A., Siddique, R., Mendis, P., Zhuge, Y., Wong, H.S., Lokuge, W., Aravinthan, T., and Schubel, P., 2021, Recycling of landfill wastes (tyres, plastics and glass) in construction – A review on global waste generation, performance, application and future opportunities, *Resour., Conserv. Recycl.*, 173, 105745.

[8] Owoeye, S.S., Jegede, F.I., and Borisade, S.G., 2020, Preparation and characterization of nano-sized silica xerogel particles using sodium silicate solution extracted from waste container glasses, *Mater. Chem. Phys.*, 248, 122915.

[9] Zhang, Y., Xia, K., Liu, X., Chen, Z., Du, H., and Zhang, X., 2019, Synthesis of cationic-modified silica gel and its adsorption properties for anionic dyes, *J. Taiwan Inst. Chem. Eng.*, 102, 1–8.

[10] Tian, G., Wang, W., Kang, Y., and Wang, A., 2016, Ammonium sulfide-assisted hydrothermal activation of palygorskite for enhanced adsorption of methyl violet, *J. Environ. Sci.*, 41, 33–43.

[11] Sarkar, S., Tiwari, N., Behera, M., Chakrabortty, S., Jhingran, K., Sanjay, K., Banerjee, S., and Tripathy, S.K., 2022, Facile synthesis, characterization and application of magnetic Fe_3O_4-coir pith composites for the removal of methyl violet from aqueous solution: Kinetics, isotherm, thermodynamics and parametric optimization, *J. Indian Chem. Soc.*, 99 (5), 100447.

[12] Onder, A., Ilgin, P., Ozay, H., and Ozay, O., 2020, Removal of dye from aqueous medium with pH-sensitive poly[(2-(acryloyloxy)ethyl]trimethylammonium chloride-co-1-vinyl-2-pyrrolidone] cationic hydrogel, *J. Environ. Chem. Eng.*, 8 (5), 104436.

[13] Altun, T., and Ecevit, H., 2022, Adsorption of malachite green and methyl violet 2B by halloysite nanotube: Batch adsorption experiments and Box-Behnken experimental design, *Mater. Chem. Phys.*, 291, 126612.

[14] Ali, N.S., Jabbar, N.M., Alardhi, S.M., Majdi, H.S., and Albayati, T.M., 2022, Adsorption of methyl violet dye onto a prepared bio-adsorbent from date seeds: Isotherm, kinetics, and thermodynamic studies, *Heliyon*, 8 (8), e10276.

[15] Astuti, W., Chafidz, A., Wahyuni, E.T., Prasetya, A., Bendiyasa, I.M., and Abasaeed, A.E., 2019, Methyl violet dye removal using coal fly ash (CFA) as a dual-site adsorbent, *J. Environ. Chem. Eng.*, 7 (5), 103262.

[16] You, X., Zhou, R., Zhu, Y., Bu, D., and Cheng, D., 2022, Adsorption of dyes methyl violet and malachite green from aqueous solution on multi-step modified rice husk powder in single and binary systems: Characterization, adsorption behavior and

physical interpretations, *J. Hazard. Mater.*, 430, 128445.

[17] Khataee, A., Fazli, A., Zakeri, F., and Joo, S.W., 2020, Synthesis of a high-performance Z-scheme 2D/2D WO_3@CoFe-LDH nanocomposite for the synchronic degradation of the mixture azo dyes by sonocatalytic ozonation process, *J. Ind. Eng. Chem.*, 89, 301–315.

[18] Fosso-Kankeu, E., Webster, A., Ntwampe, I.O., and Waanders, F.B., 2017, Coagulation/flocculation potential of polyaluminium chloride and bentonite clay tested in the removal of methyl red and crystal violet, *Arabian J. Sci. Eng.*, 42 (4), 1389–1397.

[19] Radoor, S., Kandel, D.R., Park, K., Jayakumar, A., Karayil, J., and Lee, J., 2024, Low-cost and eco-friendly PVA/carrageenan membrane to efficiently remove cationic dyes from water: Isotherms, kinetics, thermodynamics, and regeneration study, *Chemosphere*, 350, 140990.

[20] dos Santos, A.J., Brillas, E., Cabot, P.L., and Sirés, I., 2020, Simultaneous persulfate activation by electrogenerated H_2O_2 and anodic oxidation at a boron-doped diamond anode for the treatment of dye solutions, *Sci. Total Environ.*, 747, 141541.

[21] Bagtache, R., Tartaya, S., Djaballah, A.M., and Trari, M., 2022, Photocatalytic performance of $KCoPO_4$ for the methyl violet oxidation, *Chem. Phys. Lett.*, 805, 139899.

[22] Yuningsih, N.E., Ariani, L., Suprapto, S., Ulfin, I., Harmami, H., Juwono, H., and Ni'mah, Y.L., 2024, Adsorption of malachite green using activated carbon from mangosteen peel: optimization using Box-Behnken design, *J. Renewable Mater.*, 12 (5), 981–992.

[23] Katheresan, V., Kansedo, J., and Lau, S.Y., 2018, Efficiency of various recent wastewater dye removal methods: A review, *J. Environ. Chem. Eng.*, 6 (4), 4676–4697.

[24] Chen, K., Feng, Q., Ma, D., and Huang, X., 2021, Hydroxyl modification of silica aerogel: An effective adsorbent for cationic and anionic dyes, *Colloids Surf., A*, 616, 126331.

[25] Han, H., Wei, W., Jiang, Z., Lu, J., Zhu, J., and Xie, J., 2016, Removal of cationic dyes from aqueous solution by adsorption onto hydrophobic/hydrophilic silica aerogel, *Colloids Surf., A*, 509, 539–549.

[26] Madondo, N.I., and Chetty, M., 2022, Anaerobic co-digestion of sewage sludge and bio-based glycerol: Optimisation of process variables using one-factor-at-a-time (OFAT) and Box-Behnken design (BBD) techniques, *S. Afr. J. Chem. Eng.*, 40, 87–99.

[27] Wang, J., and Guo, X., 2020, Adsorption isotherm models: Classification, physical meaning, application and solving method, *Chemosphere*, 258, 127279.

[28] Myers, R.H., Montgomery, D.C., and Anderson-Cook, C.M., 2016, *Response Surface Methodology: Process and Product Optimization Using Designed Experiments*, John Wiley & Sons, Hoboken, NJ, US.

[29] Ahmad, M.A., Eusoff, M.A., Oladoye, P.O., Adegoke, K.A., and Bello, O.S., 2021, Optimization and batch studies on adsorption of methylene blue dye using pomegranate fruit peel based adsorbent, *Chem. Data Collect.*, 32, 100676.

[30] Suprapto, S., Azizah, P.A.N., and Ni'mah, Y.L., 2024, Silica gel from chemical glass bottle waste as adsorbent for methylene blue: Optimization using BBD, *J. Renewable Mater.*, 11 (12), 4007–4023.

[31] Khair, A., Putri, H.A., Suprapto, S., and Ni'mah, Y.L., 2021, The optimization of Sumbawa manganese ore beneficiation using response surface method (RSM), *AIP Conf. Proc.*, 2349 (1), 020050.

[32] Bello, O.S., Alabi, E.O., Adegoke, K.A., Adegboyega, S.A., Inyinbor, A.A., and Dada, A.O., 2020, Rhodamine B dye sequestration using *Gmelina aborea* leaf powder, *Heliyon*, 6 (1), e02872.

[33] Zhu, W., Wang, J., Wu, D., Li, X., Luo, Y., Han, C., Ma, W., and He, S., 2017, Investigating the heavy metal adsorption of mesoporous silica materials prepared by microwave synthesis, *Nanoscale Res. Lett.*, 12 (1), 323.

[34] Wang, H., Luan, W., Sun, L., Zeng, Z., Xue, W., and Bai, Y., 2022, Study on polyvinyl butyral purification process based on Box-Behnken design and artificial neural network, *Chem. Eng. Res. Des.*, 184, 291–302.

[35] Hastuti, S., Nuryono, N., and Kuncaka, A., 2015, L-arginine-modified silica for adsorption of gold(III), *Indones. J. Chem.*, 15 (2), 108–115.

[36] Kajjumba, G.W., Emik, S., Öngen, A., Özcan, H.K., and Aydın, S., 2018, "Modelling of Adsorption Kinetic Processes—Errors, Theory and Application" in *Advanced Sorption Process Applications*, Eds. Edebali, S., IntechOpen, London, UK.